Multipole-mode surface solitons

Yaroslav V. Kartashov and Lluis Torner

ICFO-Institut de Ciencies Fotoniques and Universitat Politecnica de Catalunya, Mediterranean Technology Park, 08860 Castelldefels, Barcelona, Spain

Received January 3, 2006; revised April 12, 2006; accepted April 16, 2006; posted April 18, 2006 (Doc. ID 66958)

We discover multipole-mode solitons supported by the surface between two distinct periodic lattices imprinted in Kerr-type nonlinear media. Such solitons are possible because the refractive index modulation at both sides of the interface glues together their out-of-phase individual constituents. Remarkably, we find that the new type of solitons may feature highly asymmetric shapes, and yet they are stable over wide domains of their existence, a rare property to be attributed to their surface nature. © 2006 Optical Society of America

OCIS codes: 190.5530, 190.4360, 060.1810.

Nonlinear periodic structures, or optical lattices, may support stable solitons that have no analogs, or that are highly unstable, in uniform nonlinear media. Salient examples include scalar gap, vortex, and multipole-mode solitons. Recent achievements in optical lattice induction[1–4] enabled experimental observation of such solitons. Thus the properties of vortex lattice solitons were analyzed in Ref. 5 and their experimental observation was reported in Refs. 6 and 7. Another interesting class of solutions, i.e., multipole-mode solitons, was studied theoretically in Refs. 8 and 9 and observed experimentally in Refs. 10 and 11. Bessel optical lattices also support stable multipole-mode solitons.[12–14] It was recently predicted and verified experimentally that nonlinear interfaces between periodic structures and uniform media also support solitons.[15–17] Such surface solitons are located at the very interface, and their properties depend crucially on the ratio of the refractive index of the uniform medium and mean refractive index of the periodic structure. Suitable periodic structures with engineered properties can be made in waveguide arrays with technologies currently available, and optical induction of the lattices is a potential future alternative. The power level required for the existence of surface solitons at such interfaces may be substantially reduced in comparison with that for interfaces of uniform media (see Refs. 18 and 19 for reviews) because of tunable, shallow refractive index modulations that are possible in optically induced lattices or waveguide arrays. Recently, gap surface solitons were predicted[20] and experimentally observed.[21] New types of interfaces can be produced by different lattices, opening new possibilities for exploration. In this Letter we consider the interface between two periodic lattices and show that they support multipole-mode solitons that have no analogs in uniform materials. In contrast to multipole-mode solitons in infinite periodic lattices, surface multipole solitons feature strongly asymmetric shapes, yet we found them to be stable in wide domains of their existence. Our findings constitute what we believe to be the first known example of a nontrivial soliton structure guided by a surface.

We address beam propagation at the interface produced by two lattices imprinted in a focusing medium with Kerr-type saturable nonlinearity, governed by the nonlinear Schrödinger equation for dimensionless complex amplitude of light field q:

$$i\frac{\partial q}{\partial \xi} = -\frac{1}{2}\left(\frac{\partial^2 q}{\partial \eta^2} + \frac{\partial^2 q}{\partial \zeta^2}\right) - \frac{q|q|^2}{1+S|q|^2} - R(\eta,\zeta)q. \quad (1)$$

Here the transverse η,ζ and longitudinal ξ coordinates are scaled to the beam width and diffraction length, respectively, and S is the saturation parameter. The function $R(\eta,\zeta)=\delta p H(\eta)+(p/4)[1-\cos(\Omega\eta)]\times[1-\cos(\Omega\zeta)]$ describes the refractive index profile, where p is the depth of the periodic part of the lattice, Ω is its frequency, the function $H(\eta)\equiv 0$ for $\eta\le 0$, and $H(\eta)\equiv 1$ for $\eta>0$, and δp characterizes the height of step in the constant part of the refractive index. Such refractive index landscapes might be optically induced in photorefractive crystals in which the lattice might be created by interfering four plane waves, while a nonuniform incoherent background illumination can produce a step in the refractive index profile at $\eta=0$. Other types of lattice interfaces could be realized by applying different voltages across the crystal. Equation (1) holds provided that the intensities of soliton and lattice-creating beams are small compared with the background illumination level and the crystal is biased with a strong static electric field. We stress the experimental feasibility of such setting, as well as the possibility of tuning the properties of the interface. Equation (1) holds also for nonlinear media with an imprinted refractive index modulation (see Refs. 22 and 23 for an observation of discrete solitons in waveguide arrays imprinted in saturable $LiNbO_3$ crystal and AlGaAs arrays). Equation (1) conserves the energy flow $U=\iint_{-\infty}^{\infty}|q|^2 d\eta d\zeta$.

We search for solitons with the form $q=w(\eta,\zeta)\exp(ib\xi)$, where w describes the field distribution and b is the propagation constant. The soliton profiles were found numerically with a standard relaxation method. To elucidate their linear stability we searched for perturbed solutions $q=(w+u+iv)\exp(ib\xi)$ of Eq. (1), where $u(\eta,\zeta,\xi)$ and $v(\eta,\zeta,\xi)$ are real and imaginary parts of perturbation that can grow with complex rate δ upon propagation. Linearization of Eq. (1) around w yields the following system of equations:

$$\frac{\partial v}{\partial \xi} = \frac{1}{2}\left(\frac{\partial^2 u}{\partial \eta^2} + \frac{\partial^2 u}{\partial \zeta^2}\right) - bu + \frac{3w^2 + Sw^4}{(1+Sw^2)^2}u + pRu,$$

$$\frac{\partial u}{\partial \xi} = \frac{1}{2}\left(\frac{\partial^2 v}{\partial \eta^2} + \frac{\partial^2 v}{\partial \zeta^2}\right) + bv - \frac{w^2 + Sw^4}{(1+Sw^2)^2}v - pRv, \quad (2)$$

which we solved numerically. We set $\Omega=4$, $S=0.05$, and vary the parameters b, p, and δp.

The simplest asymmetric multipole-mode solitons supported by the interface consist of two bright spots with a π phase jump between them that are located at different sides of the interface (Fig. 1). Notice that such solitons cannot exist at the interface between uniform materials because of repulsive forces acting between out-of-phase spots. Periodic refractive index modulation can compensate for repulsive forces acting between out-of-phase soliton constituents even if they have different peak amplitudes and results in multipole soliton formation. Importantly, despite the fact that the topological (phase) structure of multipole surface solitons is similar to that for multipole solitons in periodic lattices[8,9] and the twisted unstaggered modes in waveguide arrays introduced in Ref. 24 and further classified in Ref. 25, their intensity distribution can be strongly asymmetric, since the lattices forming the interface require different peak powers for self-sustained light beam propagation for a given propagation constant b. The energy flow of a dipole-mode surface soliton is a nonmonotonic function of propagation constant [Fig. 2(a)]. We found that U diverges as b approaches cutoff b_{co}, and that far from the cutoff U grows with b. In clear contrast to multipole solitons in usual periodic lattices,[8,9] the right spot of the surface soliton strongly expands over the lattice at $\eta>0$ and $\max q|_{\eta>0} \to 0$, while its left spot remains well localized as $b \to b_{co}$ [Fig. 1(a)]. The

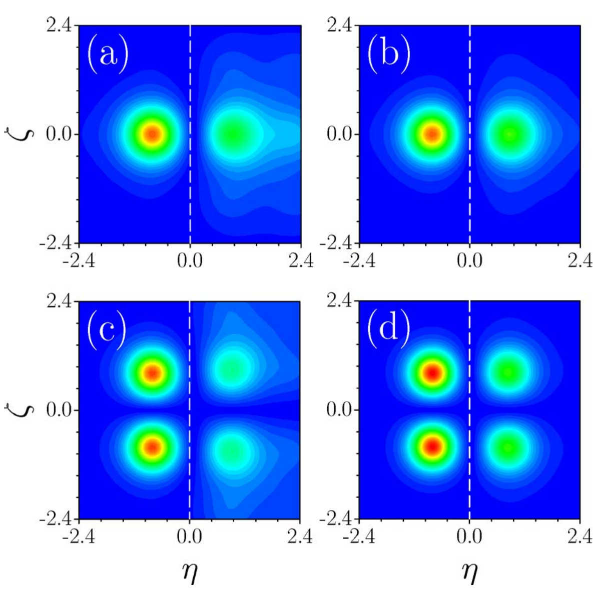

Fig. 1. (Color online) Field modulus distributions of dipole-mode surface solitons corresponding to (a) $b=3.45$ and (b) $b=4.05$ at $p=4$, $\delta p=2$ and quadrupole-mode solitons corresponding to (c) $b=5.33$ and (d) $b=7.5$ at $p=4$, $\delta p=4$. Vertical dashed lines indicate the interface position.

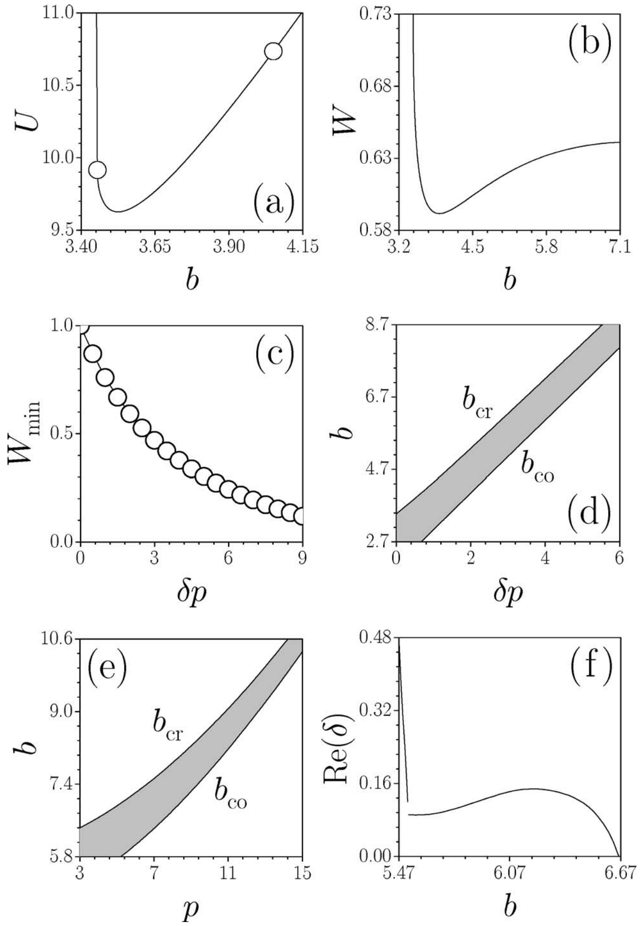

Fig. 2. (a) Total energy flow, and (b) power distribution versus propagation constant for a dipole-mode soliton at $p=4$ and $\delta p=2$. Points marked by circles in (a) correspond to solitons shown in Figs. 1(a) and 1(b). (c) Energy sharing versus δp at $p=4$. (d) Domains of stability and instability (shaded) on a $(\delta p, b)$ plane at $p=6$ and (e) on a (p,b) plane at $\delta p=4$. (f) Real part of perturbation growth rate versus propagation constant at $p=4$ and $\delta p=4$.

asymmetry in the soliton profile becomes less pronounced with an increase of b [Fig. 2(a)].

Similar behavior was encountered for other types of multipole surface solitons, including quadrupole ones, which consist of two bright spots in the region $\eta \le 0$ and two spots at $\eta>0$, while the soliton phase changes by π between different quadrants of the (η,ζ) plane [Figs. 1(c) and 1(d)]. The power distribution $W=U_r/U_l$, defined as the ratio between the power U_r localized at $\eta>0$ and the power U_l localized at $\eta \le 0$, diverges as $b \to b_{co}$, since $U_r(b\to b_{co}) \to \infty$, while U_l remains finite [Fig. 2(b)]. The quantity W characterizes the degree of asymmetry of the light intensity distribution of the surface soliton. Notice the clearly pronounced minimum in the dependence $W(b)$. Figure 1(c) shows that W_{min} decreases with an increase of the height δp of step in the refractive index, which indicates a progressive asymmetry growth.

We found that for the fixed lattice depth, the cutoff, b_{co} increases almost linearly with δp [Fig. 2(d)]. In contrast, for fixed δp the dependence $b_{co}(p)$ is nonmonotonic, as b_{co} tends to infinity for $p\to 0$ and

$p \to \infty$. Figure 2(e) shows part of the dependence $b_{co}(p)$ for $p > 3$. Importantly, linear stability analysis revealed that surface solitons become completely stable when the propagation constant exceeds a critical value $b_{cr} > b_{co}$. The width of the instability domain remains almost unchanged with an increase of δp, i.e., with an increase of asymmetry in the soliton profile [Fig. 2(d)], and it decreases with an increase of lattice depth p [Fig. 2(e)]. Thus even moderate periodic refractive index modulation can stabilize highly asymmetric multipole surface solitons. We found that, similarly to weakly localized twisted modes in waveguide arrays,[24] the largest part of the instability domain for surface multipole solitons is associated with oscillatory instabilities $[\mathrm{Re}(\delta)\mathrm{Im}(\delta) \neq 0]$, while close to the cutoff surface solitons are exponentially unstable [Fig. 2(f)]. Notice that oscillatory instability in the low-power limit is a characteristic signature of multipole solitons existing in different physical systems. Increasing the lattice depth suppresses the instability, and it is accompanied by a reduction of the maximal value of $\mathrm{Re}(\delta)$.

The results of the linear stability analysis were fully confirmed by direct simulations of Eq. (1). We used input conditions with $q|_{\xi=0} = w(\eta,\zeta)[1+\rho(\eta,\zeta)]$, in which $\rho(\eta,\zeta)$ described white noise with a Gaussian distribution and variance $\sigma^2_{\mathrm{noise}}$. In all cases, solitons with $b > b_{cr}$ perturbed with considerable input noise survived over huge distances (Fig. 3). A decay of unstable solitons typically results in emission of part of the power localized in the region $\eta > 0$ and the formation of the soliton in the region $\eta \leq 0$. Simulations show that asymmetric surface solitons can be excited by Gaussian beams with properly selected amplitudes and phases, which confirms the robustness of the solitons. Finally, besides dipole and quadrupole solitons, we have also found a variety of more complex stable asymmetric solitons (not shown here) supported by the interface between two lattices.

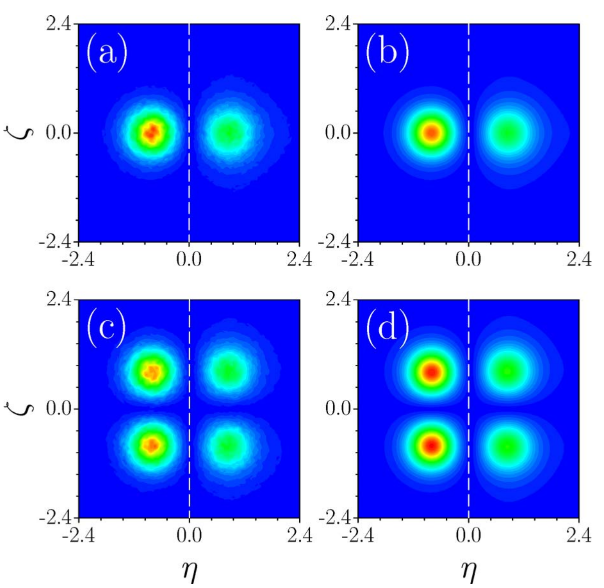

Fig. 3. (Color online) Stable propagation of a dipole-mode soliton with $b=7$ and a quadrupole-mode soliton with $b=7.5$ in the presence of white input noise with variance $\sigma^2_{\mathrm{noise}}=0.01$. Field modulus distributions are shown at (a), (c) $\xi=0$ and (b), (d) $\xi=256$. In all cases $p=4$, $\delta p=4$.

Y. Kartashov's e-mail address is Yaroslav.Kartashov@icfo.es.

References

1. J. W. Fleischer, T. Carmon, M. Segev, N. K. Efremidis, and D. N. Christodoulides, Phys. Rev. Lett. **90**, 023902 (2003).
2. J. W. Fleischer, M. Segev, N. K. Efremidis, and D. N. Christodoulides, Nature **422**, 147 (2003).
3. D. Neshev, E. Ostrovskaya, Y. Kivshar, and W. Krolikowski, Opt. Lett. **28**, 710 (2003).
4. H. Martin, E. D. Eugenieva, Z. Chen, and D. N. Christodoulides, Phys. Rev. Lett. **92**, 123902 (2004).
5. J. Yang and Z. Musslimani, Opt. Lett. **28**, 2094 (2003).
6. D. N. Neshev, T. J. Alexander, E. A. Ostrovskaya, Y. S. Kivshar, H. Martin, I. Makasyuk, and Z. Chen, Phys. Rev. Lett. **92**, 123903 (2004).
7. J. W. Fleischer, G. Bartal, O. Cohen, O. Manela, M. Segev, J. Hudock, and D. N. Christodoulides, Phys. Rev. Lett. **92**, 123904 (2004).
8. Z. H. Musslimani and J. Yang, J. Opt. Soc. Am. B **21**, 973 (2004).
9. Y. V. Kartashov, A. A. Egorov, L. Torner, and D. N. Christodoulides, Opt. Lett. **29**, 1918 (2004).
10. J. Yang, I. Makasyuk, A. Bezryadina, and Z. Chen, Opt. Lett. **29**, 1662 (2004).
11. J. Yang, I. Makasyuk, P. G. Kevrekidis, H. Martin, B. A. Malomed, D. J. Frantzeskakis, and Z. Chen, Phys. Rev. Lett. **94**, 113902 (2005).
12. Y. V. Kartashov, V. A. Vysloukh, and L. Torner, Phys. Rev. Lett. **93**, 093904 (2004).
13. Y. V. Kartashov, A. A. Egorov, V. A. Vysloukh, and L. Torner, J. Opt. B: Quantum Semiclassical Opt. **6**, 444 (2004).
14. Y. V. Kartashov, A. A. Egorov, V. A. Vysloukh, and L. Torner, Phys. Rev. E **70**, 065602(R) (2004).
15. K. G. Makris, S. Suntsov, D. N. Christodoulides, G. I. Stegeman, and A. Hache, Opt. Lett. **30**, 2466 (2005).
16. J. Hudock, S. Suntsov, D. N. Christodoulides, and G. I. Stegeman, Opt. Express **13**, 7720 (2005).
17. S. Suntsov, K. G. Makris, D. N. Christodoulides, G. I. Stegeman, A. Hache, R. Morandotti, H. Yang, G. Salamo, and M. Sorel, Phys. Rev. Lett. **96**, 063901 (2006).
18. H. E. Ponath and G. I. Stegeman, eds., *Nonlinear Surface Electromagnetic Phenomena* (North-Holland, 1991).
19. G. I. Stegeman, E. M. Wrigth, N. Finlayson, R. Zanoni, and C. T. Seaton, J. Lightwave Technol. **6**, 953 (1988).
20. Y. V. Kartashov, V. A. Vysloukh, and L. Torner, Phys. Rev. Lett. **96**, 073901 (2006).
21. C. R. Rosberg, D. N. Neshev, W. Krolikowski, A. Mitchell, R. A. Vicencio, M. I. Molina, and Y. S. Kivshar, arXiv:physics/0603202 (2006).
22. F. Chen, M. Stepic, C. E. Rüter, D. Runde, D. Kip, V. Shandarov, O. Manela, and M. Segev, Opt. Express **13**, 4314 (2005).
23. J. Meier, G. Stegeman, D. Christodoulides, R. Morandotti, M. Sorel, H. Yang, G. Salamo, J. Aitchison, and Y. Silberberg, Opt. Express **13**, 1797 (2005).
24. S. Darmanyan, A. Kobyakov, and F. Lederer, JETP **86**, 682 (1998).
25. G. Kalosakas, arXiv.org, nlin.PS/0512028 (2005).